#### RESEARCH



# Marine sulfated glycans inhibit the interaction of heparin with S-protein of SARS-CoV-2 Omicron XBB variant

Peng He<sup>1,2</sup> · Yuefan Song<sup>1,3</sup> · Weihua Jin<sup>1,4</sup> · Yunran Li<sup>1,3</sup> · Ke Xia<sup>1,3</sup> · Seon Beom Kim<sup>5,6</sup> · Rohini Dwivedi<sup>5</sup> · Marwa Farrag<sup>5</sup> · John Bates<sup>5</sup> · Vitor H. Pomin<sup>5</sup> · Chunyu Wang<sup>1,3</sup> · Robert J. Linhardt<sup>1,3,7</sup> · Jonathan S. Dordick<sup>1,7</sup> · Fuming Zhang<sup>1,7</sup>

Received: 18 December 2023 / Revised: 26 March 2024 / Accepted: 4 April 2024 / Published online: 20 April 2024 © The Author(s), under exclusive licence to Springer Science+Business Media, LLC, part of Springer Nature 2024

#### **Abstract**

The severe acute respiratory syndrome coronavirus 2 (SARS-CoV-2) has caused a worldwide COVID-19 pandemic, leading to 6.8 million deaths. Numerous variants have emerged since its outbreak, resulting in its significantly enhanced ability to spread among humans. As with many other viruses, SARS-CoV-2 utilizes heparan sulfate (HS) glycosaminoglycan (GAG) on the surface of host cells to facilitate viral attachment and initiate cellular entry through the ACE2 receptor. Therefore, interfering with virion-HS interactions represents a promising target to develop broad-spectrum antiviral therapeutics. Sulfated glycans derived from marine organisms have been proven to be exceptional reservoirs of naturally existing HS mimetics, which exhibit remarkable therapeutic properties encompassing antiviral/microbial, antitumor, anticoagulant, and anti-inflammatory activities. In the current study, the interactions between the receptor-binding domain (RBD) of S-protein of SARS-CoV-2 (both WT and XBB.1.5 variants) and heparin were applied to assess the inhibitory activity of 10 marine-sourced glycans including three sulfated fucans, three fucosylated chondroitin sulfates and two fucoidans derived from sea cucumbers, sea urchin and seaweed Saccharina japonica, respectively. The inhibitory activity of these marine derived sulfated glycans on the interactions between RBD of S-protein and heparin was evaluated using Surface Plasmon Resonance (SPR). The RBDs of S-proteins from both Omicrion XBB.1.5 and wild-type (WT) were found to bind to heparin, which is a highly sulfated form of HS. All the tested marine-sourced sulfated glycans exhibited strong inhibition of WT and XBB.1.5 S-protein binding to heparin. We believe the study on the molecular interactions between S-proteins and host cell glycosaminoglycans provides valuable insight for the development of marine-sourced, glycan-based inhibitors as potential anti-SARS-CoV-2 agents.

Keywords Marine sulfated glycans · SARS-CoV-2 · Omicron XBB.1.5 · Spike Protein · Heparin · SPR

- ☑ Jonathan S. Dordick dordick@rpi.edu
- ☐ Fuming Zhang zhangf2@rpi.edu
- Center for Biotechnology and Interdisciplinary Studies, Rensselaer Polytechnic Institute, Troy, NY, USA
- School of Oceanography, Beibu Gulf University, 535011 Oinzhou, China
- Department of Chemistry and Chemical Biology, Rensselaer Polytechnic Institute, 12180 Troy, NY, USA

- College of Biotechnology and Bioengineering, Zhejiang University of Technology, 310014 Hangzhou, China
- Department of BioMolecular Sciences, Research Institute of Pharmaceutical Sciences, The University of Mississippi, Oxford, MS, USA
- Department of Food Science & Technology, College of Natural Resources and Life Science, Pusan National University, Miryang, Republic of Korea
- Departments of Chemical and Biological Engineering, Rensselaer Polytechnic Institute, 12180 Troy, NY, USA



### Introduction

At the end of 2019, a contagious novel coronavirus, SARS-CoV-2, originated and rapidly disseminated across the world, resulting in the pandemic of COVID-19. As of April 2023, there were over 762 million confirmed cases and more than 6.8 million deaths attributed to SARS-CoV-2 based on data from WHO Coronavirus (COVID-19) Dashboard (https://covid19.who.int/). Multiple COVID-19 pandemic waves have occurred accompanied by numerous new SARS-CoV-2 variants. According to Centers for Disease Control and Prevention (CDC) of the US, COVID-19 was reported as the fourth leading cause of death in the United States in 2022. This virus exhibits a high mutation rate with a positive-sense single-stranded RNA [1]. Mutations on the S-protein of SARS-CoV-2, which performs vital functions in the attachment and entry of SARS-CoV-2 into host cell, have led to five circulating variants of concern (VOC) -Alpha, Beta, Gamma, Delta and multiple Omicron variants [2].

Among the Omicron variants, XBB.1.5 has been spreading rapidly worldwide during the last several months. As of April 2023, the highly transmissible XBB.1.5 variant was projected to represent approximately 78% of US infections according to the CDC. The Omicron XBB.1.5 is a lineage that has descended from the XBB (a recombinant of BA.2.10.1 and BA.2.75) family with two mutations (G252V and F486P) in the S-protein [3]. The presence of the uncommon F486P mutation in XBB.1.5 seems to be associated with the strength of interaction between the receptor-binding domain (RBD) of the S-protein and human angiotensinconverting enzyme-2 (hACE2) complexes, enhancing the ability of the virus to spread [4]. The higher ACE2 binding affinity and the ability to escape from current monoclonal antibodies accelerated the dominance of XBB.1.5 in many countries.

Anionic glycans such as heparan sulfate (HS), chondroitin sulfates (CS), keratan sulfates (KS), hyaluronan and sialic acids are widely distributed in mammalian tissues [5]. Those anionic glycans serve as facilitators (and sometimes as receptors/co-receptors) to promote pathogen attachment, invasion, assembly, and release to host cells [6-7]. Many studies have demonstrated that HS, a significant constituent of the glycocalyx found in mammalian cells, interacts with SARS-CoV-2 S-protein aiding the virus in infiltrating host cells [8–10]. Therefore, molecules that interfere with the binding of S-protein to HS have shown effectiveness against SARS-CoV-2. Marine sulfated glycans garnered significant interest as antiviral drug candidates due to their excellent antiviral activity, low cytotoxicity, green renewable sources, and low production costs [11-12]. We have shown that some marine sulfated glycans exhibit high inhibition activity to previous SARS-CoV-2 strains, like WT, Delta, and Omicron, by interfering with the binding of viral S-protein to host cell [13–16].

In the current study, the binding of XBB.1.5 S-protein RBDs to heparin (a highly sulfated HS) was analyzed in comparison with the WT version using SPR. A collection of marine glycans (sulfated fucans, as well as fucosylated chondroitin sulfates derived from marine echinoderm and seaweed, Fig. 1) and two desulfated derivatives, were prepared to investigate the inhibitory activity of XBB.1.5 S-protein-heparin interactions. We observe that both WT and XBB.1.5 S-protein RBDs bind to heparin with high affinity, and the interactions can be inhibited by several marine-sourced sulfated glycans.

### **Materials and methods**

#### **Materials**

Eight marine glycans, IbSF, desIbSF, IbFucCS, desIbFucCS, PpFucCS, LvSF, HfSF, and HfFucCS, were purified from sea cucumbers I. badionotus and P. pygmaea, sea urchin L. variegatus, and the Florida sea cucumber H. floridana, in Dr. Pomin's laboratory at the University of Mississippi. Two fucoidans (RPI-27 and RPI-28) were purified in Dr. Jin's Lab from seaweed Saccharina japonica. The SARS-CoV-2 S-protein RBD wild-type (WT) was expressed in Expi293F cells in Bates lab at the University of Mississippi. The S-protein RBD XBB.1.5 of SARS-CoV-2 was purchased from Sino Biological Inc. (Wayne, PA, USA). The recombinant wild-type S-protein RBD is composed of 234 amino acids and is estimated to have a molecular weight of 26.72 kDa. The recombinant XBB.1.5 S-protein RBD is composed of 234 amino acids and is estimated to have a molecular weight of 26.58 kDa (see the amino acid sequences in Fig. 2). Porcine intestinal heparin with an average molecular weight of 15 kDa was from Celsus Laboratories (Cincinnati, OH, USA). Streptavidin (SA) sensor chips were purchased from Cytiva (Uppsala, Sweden). SPR measurements were conducted using a BIAcore T200 or 3000 SPR instrument (Cytiva, Uppsala, Sweden). SPR data processing was carried out using Biaevaluation software, version 4.0.1 or 3.2.

### **Heparin SPR chip preparation**

Biotinylated heparin: a solution was prepared by combining 500  $\mu$ g of heparin and 500  $\mu$ g of amine-PEG<sub>3</sub>-Biotin (Thermo Scientific, Waltham, MA, USA) in 100  $\mu$ L of water, following 2.5 mg NaCNBH<sub>3</sub> was added to start the reaction. The reaction was at 70 °C for 24 h, then additional



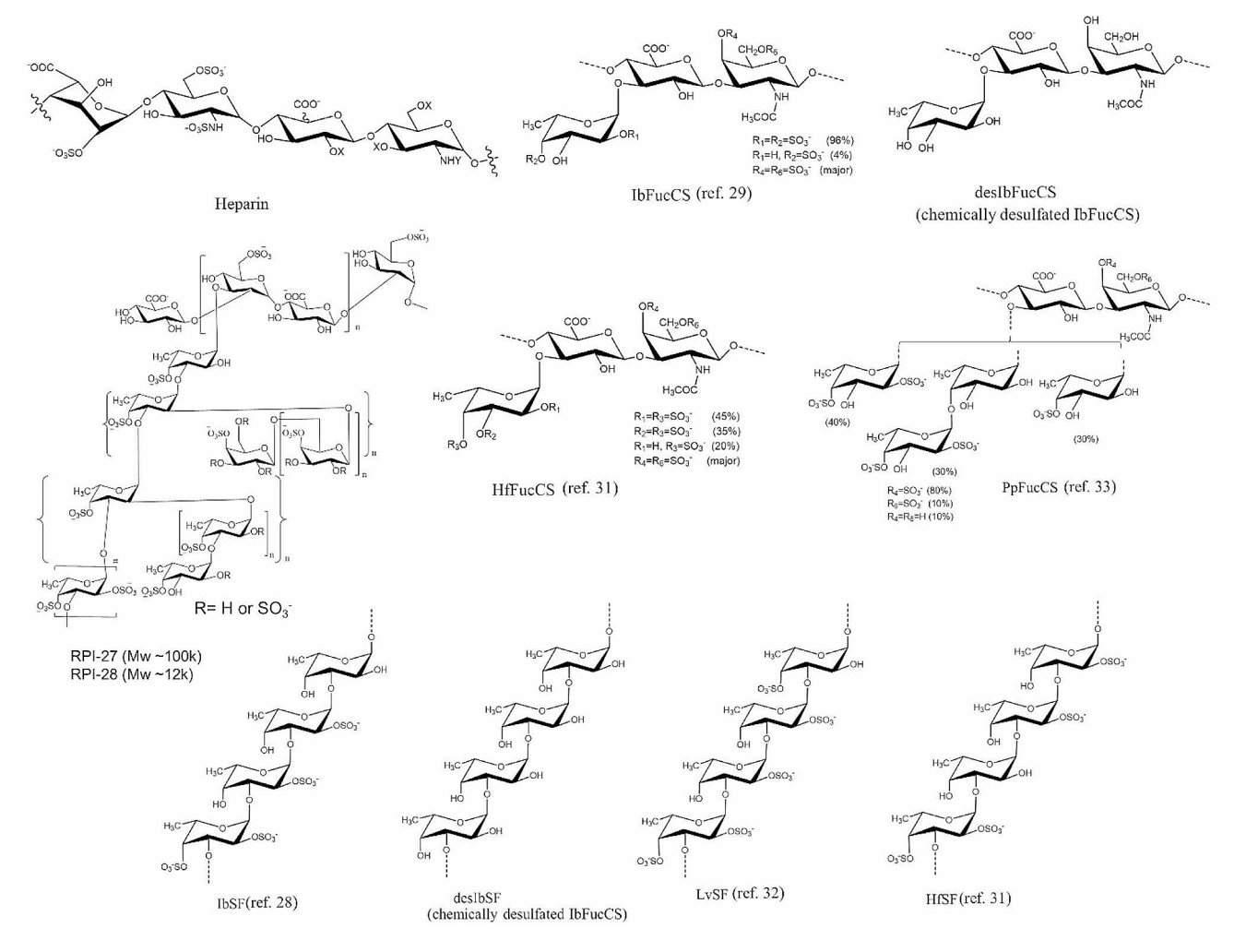


Fig. 1 Chemical structures of heparin and marine sulfated glycans

2.5 mg NaCNBH $_3$  was added to continue the reaction for 24 h. Once the reaction was finished, the biotinylated heparin was desalted using a 3000 molecular weight cut-off membrane and freeze dried. The following procedure was employed to make heparin chip by immobilizing heparin on SA surface: Flow cells 2 to 4 were carefully infused with a solution of biotinylated heparin (0.1 mg/mL) in HBS-EP $^+$  buffer, with a volume of 20  $\mu$ L at a flow rate of 10  $\mu$ L/min. A reference flow cell 1 was prepared by an injection of 20  $\mu$ L of saturated biotin.

# Binding kinetics and affinity measurement on interaction between S-protein RBD and heparin

The S-protein RBDs were diluted in HBS-EP+ buffer (150 mM NaCl, 10 mM HEPES, 0.05% v/v Surfactant P20, pH, 7.4). Various concentrations of S-protein RBD were injected at a flow rate of 30  $\mu$ L/min. After each injection, a consistent buffer was directed flowed over the sensor surface for a duration of 3 min to perform dissociation. To regenerate the

SPR chip, a volume of 30  $\mu$ L of 2 M NaCl was injected into each channel. All responses were monitored as sensorgrams at 25  $^{\circ}$ C.

### Inhibitory effects of the marine sulfated glycans on the interactions between heparin and the S-protein RBD

To assess the inhibitory activity between the S-protein RBD and heparin, a mixture of S-protein RBD at a concentration of 1  $\mu$ M and various glycans at a concentration of 5  $\mu$ g/mL was prepared in HBS-EP<sup>+</sup> buffer (pH 7.4). The mixture was then injected to the heparin chip at a flow rate of 30  $\mu$ L/min. A NaCl solution (2 M) was injected in a volume of 30  $\mu$ L to regenerate the sensor surface after each binding analysis.



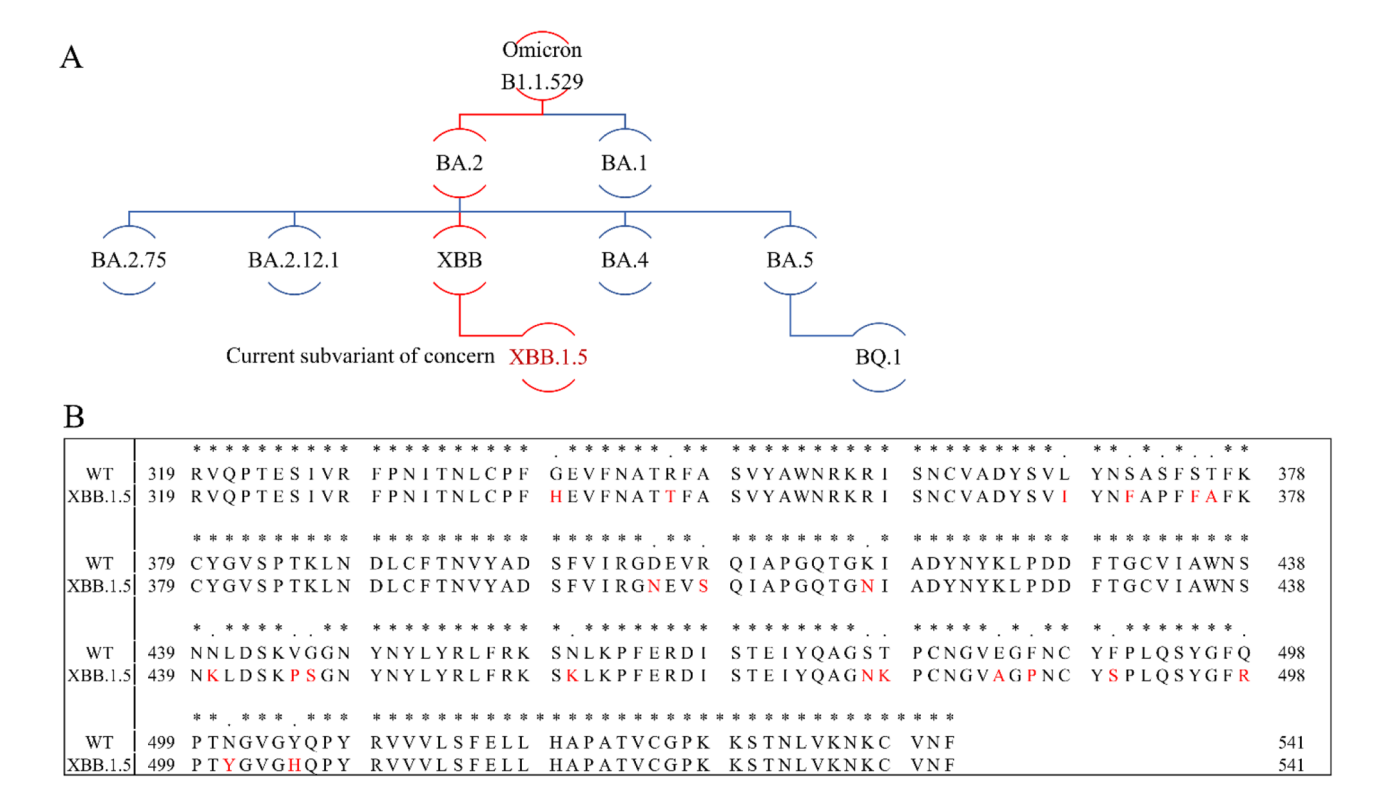


Fig. 2 Omicron phylogenetic tree and S-protein RBD amino acid multiple sequence alignment. (A) Omicron phylogenetic tree, adapted from Nextstrain and CoVariants. (B) Mutation profile of S-protein

### **Results and discussion**

# Mutations in XBB S-protein RBD and variants of SARS-CoV-2

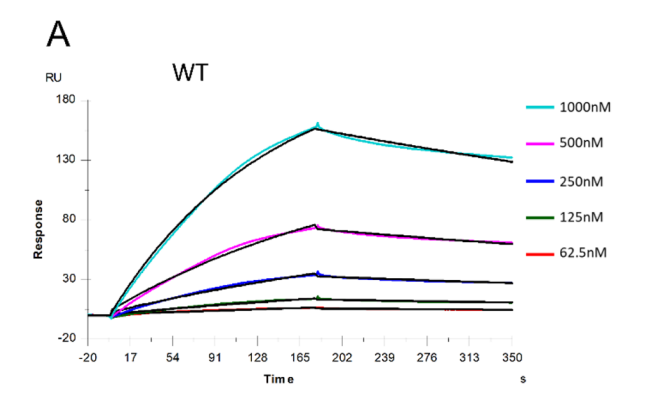
Throughout the pandemic of COVID-19, numerous SARS-CoV-2 variants have shown up and posed weighty challenges to both human health and global healthcare systems. Several of these variants pose a significant threat due to their heightened transmissibility, reduced vaccine and antibody effectiveness and increased virulence. Five variants of concern (VOC) have been declared by the WHO, namely Alpha, Beta, Gamma, Delta and Omicron. Omicron was named in November 2021 after being detected in both South Africa and Botswana. Studies showed that this variant has many mutations leading to an increased risk of reinfection and transmissibility [17-18]. Omicron rapidly spread worldwide and became the main variant. As the pandemic evolved, a number of new Omicron subvariants emerged, including BA.1, BA.2, BA.2.75, BA.2.12.1, BA.4, BA.5 and XBB (Fig. 2A). XBB emerged and rose to prominence in India and Singapore in September 2022, and soon thereafter this variant became the dominant variant in several countries [19]. By the end of 2022, XBB's sublineage XBB.1.5 outcompeted other VOCs, and became the most dominant RBD of WT and XBB.1.5 strains. Multiple sequence alignment was carried out by Clustal Omega (1.2.4). Asterisks (\*) indicate positions with a single, fully conserved residue

variant in the USA. Sequence comparison between WT and XBB.1.5 showed that 21 amino acid mutations emerged in the S-protein RBD (Arg319-Phe541, Fig. 2B). Among these amino acid mutations, XBB.1.5 harbors an F486P mutation, which enables the XBB.1.5 outcompete other Omicron variants.

# Binding kinetics and affinity measurement of heparin-SARS-CoV-2 S-proteins interactions

Heparin/HS is a group of highly sulfated, polydisperse, linear polysaccharides which consist of variably repeating disaccharide building blocks, D-glucuronic acid (GlcA) or L-iduronic acid linked to N-acetylated or N-sulfated glucosamine [20]. Heparin/HS can be widely found throughout the extracellular matrix, as well as on the surfaces of mammalian cells. Through binding and regulating a wide range of proteins, heparin/HS regulates various biological processes, such as blood coagulation, tumor metastasis and pathogen invasion [21]. Heparan sulfates are covalently attached to various core proteins presented in the extracellular matrix and on the cell surfaces, forming HS proteoglycans (HSPGs), which play critical roles in pathogen infection, especially in cellular attachment. Many studies suggest that the highly negatively charged and ubiquitously





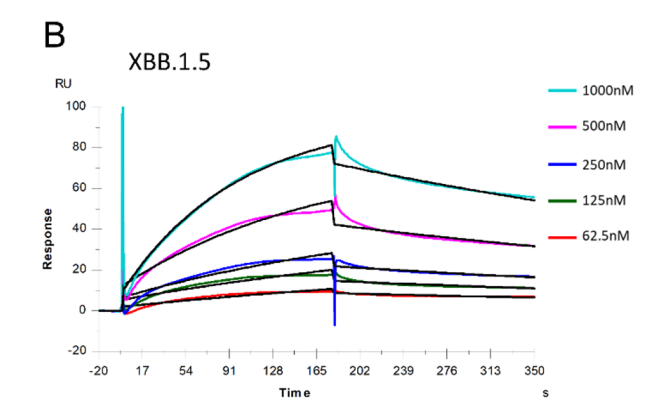


Fig. 3 SPR sensorgrams of S-protein RBD of WT and XBB.1.5 binding to heparin. SPR sensorgrams of S-protein RBD binding with heparin; (A) WT and (B) XBB.1.5. Concentrations of S-protein RBD (from top to bottom) are 1000, 500, 250, 125, and 63 nM, respectively

Table 1 Kinetic data of interactions of S-protein RBD of WT and XBB 1.5 with heparin

	o with meparin		
	$k_a(M^{-1}s^1)$	$k_d(1/s)$	$K_D(M)$
WT	$3.3 \times 10^{3}$	$1.2 \times 10^{-3}$	$3.5 \times 10^{-7}$
	$(\pm 21)*$	$(\pm 4.1 \times 10^{-6})^*$	$(\pm 4.0 \times 10^{-8}) **$
XBB	$2.1 \times 10^4$	$3.4 \times 10^{-3}$	$1.6 \times 10^{-7}$
	$(\pm 250)*$	$(\pm 2.3 \times 10^{-5})$ *	$(\pm 2.9 \times 10^{-8})$ **

<sup>\*</sup> The data with (±) in parentheses are the standard deviations (SD) from global fitting of five injections. \*\*Standard deviation (SD) on triplicated experiments

expressed HSPGs provide an ideal adhesive primary attachment point for viruses [22–25]. Heparin, the highest sulfated GAG, is well studied as an anticoagulant, and heparin and its analogs are inhibitors to different viruses through blocking viral-HSPGs interactions. Our previous studies showed that full-length heparin and its oligomers can interact with some viral proteins, such as monkeypox A35/A29 proteins, SARS-CoV-2 S-proteins and the glycoproteins of respiratory syncytial virus [16, 26–27]. In this study, a SPR chip immobilized with heparin was prepared to assess the binding kinetics of heparin and S-protein interactions using S-protein RBD from WT and XBB.1.5 variants. Sensorgrams for interactions of heparin with these two S-protein RBDs are presented in Fig. 3.

The association and dissociation rates (ka and kd) as well as the binding equilibrium dissociation constant ( $K_D = \text{ka/kd}$ ) were used to evaluate the interaction between the SARS-CoV-2 S-protein RBD (wild-type and XBB.1.5 variant) and heparin. The interaction kinetics were analyzed using a 1:1 Langmuir binding model, and the results are presented in Table 1. The binding affinities of S-protein RBD with heparin are nanomolar: XBB.1.5 ( $K_D = 160 \text{ nM}$ ) is slightly stronger than WT ( $K_D = 350 \text{ nM}$ ). From Fig. 2 we can find that among these 20 mutations on S-protein RBD region, half of the mutations result in reduced amino acid hydrophilicity, while others enhanced the hydrophilicity. Among amino

acids from N440 to T500, there are nine mutations, eight of which enhance hydrophilicity. Notably, F486P is known to aid the virus escape the immune system's detection. Interactions between protein and heparin are mainly based on the electrostatic attraction, and therefore, negatively charged GAGs are expected to interact with positively charged amino acids such as lysine (K), arginine (R), and histidine (H). Comparing the sequences of S-protein of XBB with WT (Fig. 2), an additional six positively charged amino acid residues are found on the XBB RBD, which can enhance heparin binding affinity. Based on the theoretical binding modeling of the Omicron S protein RBD and heparin oligosaccharides using AutoDock Vina, the amino acid residues, such as R355, R577 and R357 in BA.2.12.1 RBD and R346, K440, K444 in BA.4/BA.5 RBD, make up a potential binding sites for heparin and heparan sulfate [27].

## Inhibitory activity of *Isostichopus badionotus*sourced sulfated glycans, IbSF, IbSFucCS on S-protein RBD binding to heparin

Sulfated fucan (IbSF) and fucosylated chondroitin sulfate (IbSFucCS) from sea cucumber *I. badionotus*, initially identified by Chen et al. [28–29]. (see structures in Fig. 1). Both IbSF and IbFucCS demonstrated effective anticoagulant and antithrombotic activities. Our previous study demonstrated that these two marine sulfated glycans also were promising inhibitors towards monkeypox virus (MPXV). The desulfated forms of IbSF and IbFucCS (desIbSF desIbFucCS) were prepared as described previously [30], and showed weak competitive inhibition activity between surface heparin and A29 and A35 proteins of [16]. Pomin's group indicated that IbSF and IbFucCS showed excellent SARS-CoV-2 inhibition activity on both WT and Delta variants, by disrupting the binding of virus on the surface of host cells [15].



SPR solution/surface competition experiments were used to test the ability of *I. badionotus*-derived glycans (IbFucCS, IbSF, and the desulfated analogues desIbFucCS and desIbSF) to inhibit the interactions between RBD of S-proteins (WT and XBB.1.5) and immobilized heparin (Fig. 4A, C). 1 µM RBD proteins were premixed with Ib glycans (5 µg/mL) (WT and XBB.1.5 individually) and injected to heparin chip. Both Ib-sourced sulfated glycans, IbSF and IbFucCS, significantly inhibited the binding of surface-immobilized heparin to the RBD of S-proteins (WT and XBB.1.5). Soluble heparin demonstrated a 53.4% and 54.6% reduction in the binding of the WT and XBB.1.5 variants of the SARS-CoV-2 S-protein, respectively, to heparin immobilized on the surface. (Fig. 4B, D). IbSF and IbFucCS exhibited a higher inhibition activity of WT S-protein binding to immobilized heparin, with 94.8% and 99.5%, respectively. At the same time, IbSF and IbFucCS, also demonstrated a high level of inhibitory effectiveness, with normalized XBB. 1.5 ratio of 92.5% and 91.3%, respectively. The chemically desulfated derivatives, desIbSF and desIbFucCS, exhibited significantly lower competitive inhibition of heparin binding to both WT and XBB.1.5 S-proteins. Our results indicate that sulfation of these marine-sourced glycans perform an important role in the interaction of S-proteins.

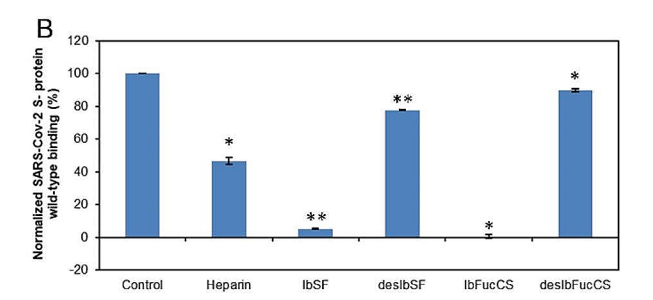
## Α Control 130 Heparin IbSF 80 deslbSF IbFucCS 30 deslbFucCS $\mathbf{C}_{_{\mathsf{RU}}}$ 100 80 Contro Heparin IbSF deslbSF IbFucCS deslbFucCS 350

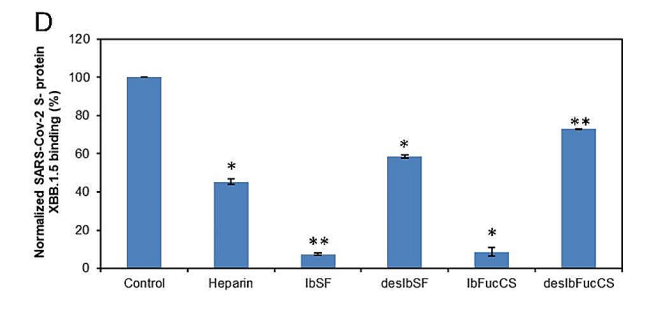
Fig. 4 Solution competition between heparin and Ib glycans. (A) SPR sensorgrams of the WT SARS-CoV-2 S-protein RBD—heparin interaction competing with different Ib glycans. The concentration of the WT SARS-CoV-2 S-protein RBD was 1  $\mu M$  mixed with 5  $\mu g/mL$  of different Ib glycans. (B) Bar graphs (based on triplicate experiments with standard deviation) of normalized WT SARS-CoV-2 S-protein RBD binding preference to surface heparin by competing with different Ib glycans. (C) SPR sensorgrams of the XBB.1.5 SARS-CoV-2 S-protein

# Inhibitory activity of *Holothuria floridana*-sourced glycans, HfSF and HfFucCS on S-protein RBD binding to heparin

HfSF and HfFucCS, from the sea cucumber *H. floridana* were first reported by Shi et al. 2019 [31] (see structures in Fig. 1). Excellent inhibitory activities against certain SARS-CoV-2 variants and MPXV were observed for these Hf derived glycans [15, 16]. (Dwivedi et al., 2022; He et al., 2023).

Again, we used solution/surface competition SPR to examine the effectiveness of HfSF and HfFucCS in inhibiting the interactions between RBD of S-proteins (WT and XBB.1.5) and heparin. 5 μg/mL of these Hf derived glycans was premixed with 1 μM S-proteins (WT and XBB.1.5 individually) and injected to heparin chip. Solution competition SPR results are indicated in Fig. 5A, C. Heparin reduced the binding of WT and XBB.1.5 S-proteins to surface-immobilized heparin by 53.4% and 54.5% correspondingly. HfSF and HfFucCS exhibited remarkable efficacy in inhibiting the binding of wild-type S-protein to heparin immobilized on the surface, demonstrating percentages of 88.9% and 93.1%, respectively. Meanwhile, HfSF and HfFucCS also showed good results for the inhibitions of



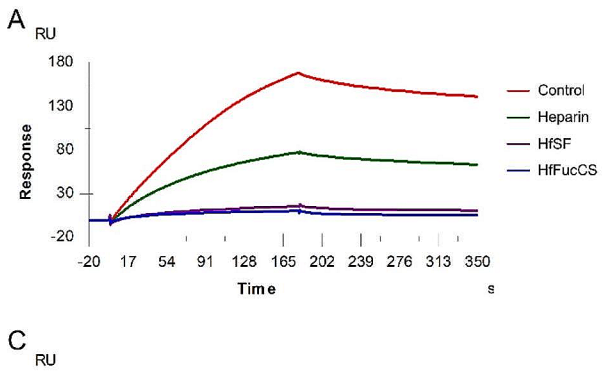


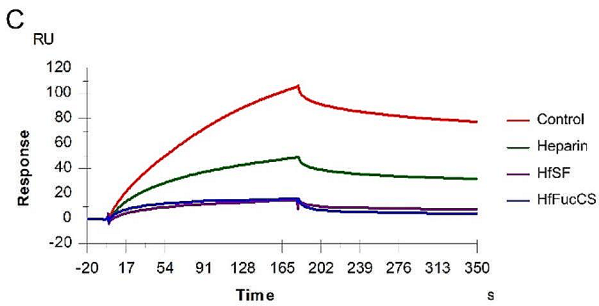
RBD–heparin interaction competing with different Ib glycans. The concentration of the the XBB.1.5 SARS-CoV-2 S-protein RBD was 1  $\mu$ M mixed with 5  $\mu$ g/mL of different Ib glycans. (**D**) Bar graphs (based on triplicate experiments with standard deviations) of the normalized XBB.1.5 SARS-CoV-2 S-protein RBD binding preference to surface heparin by competing with different Ib glycans. Statistical analysis was performed using an unpaired two-tailed t-test (\*:  $p \le 0.05$  compared with the control, \*\*:  $p \le 0.01$  compared with the control)

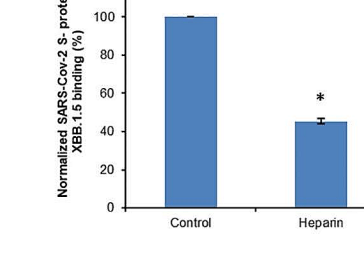


HfFucCS

HfFucCS







Control

В

100

80

60

40

20

0

Normalized SARS-Cov-2 S- protein wild-type binding (%)

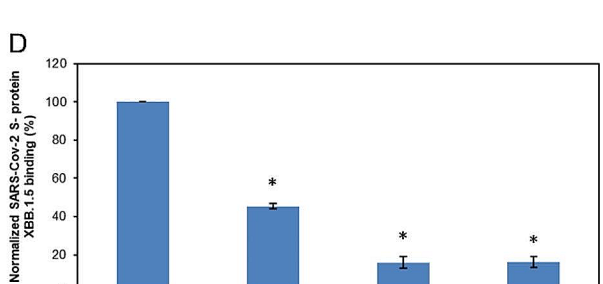
Fig. 5 Solution competition between heparin and Hf glycans. (A) SPR sensorgrams of the WT SARS-CoV-2 S-protein RBD-heparin interaction competing with different Hf glycans. The concentration of the WT SARS-CoV-2 S-protein RBD was 1 µM mixed with 5 µg/mL of different Hf glycans. (B) Bar graphs (based on triplicate experiments with standard deviation) of normalized WT SARS-CoV-2 S-protein RBD binding preference to surface heparin by competing with different Hf glycans. (C) SPR sensorgrams of the XBB.1.5 SARS-CoV-2 S-protein

XBB.1.5 S-protein binding to heparin immobilized on the surface, with 84.0% and 83.8%, respectively (Fig. 5B, D).

### Inhibitory activity of sulfated glycans, LvSF and **PpFucCS on S-protein RBD binding to heparin**

Sulfated fucan LvSF is a polysaccharide extracted from Lytechinus variegatus a species of sea urchin [32], while the fucosylated chondroitin sulfate PpFucCS is extracted from Pentacta pygmaea, a species of sea cucumber (see structures in Fig. 1) [33].

To perform solution/surface competition SPR, 5 μg/mL glycans (LvSF or PpFucCS) was premixed with 1 µM RBD of S-proteins (WT and XBB.1.5). Solution competition results between these marine-sourced glycans and heparin are shown in Fig. 6A, C. PpFucCS and LvSF exhibited remarkable efficacy in inhibiting the binding of WT S-protein to surface-immobilized heparin, demonstrating 97.9% and 86.0% respectively. Meanwhile, PpFucCS and LvSF demonstrated excellent outcomes inhibiting the binding of XBB.1.5 S-protein to heparin immobilized on the surface, achieving inhibitions of 91.5% and 88.6% respectively. (Fig. 6B, D).



Heparin

RBD-heparin interaction competing with different Hf glycans. The concentration of the XBB.1.5 SARS-CoV-2 S-protein RBD was 1 uM mixed with 5 µg/mL of different Hf glycans. (D) Bar graphs (based on triplicate experiments with standard deviations) of the normalized XBB.1.5 SARS-CoV-2 S-protein RBD binding preference to surface heparin by competing with different Hf glycans. Statistical analysis was performed using an unpaired two-tailed t-test (\*:  $p \le 0.05$  compared with the control)

HfSF

### Inhibitory activity of fucoidans: RPI-27 and RPI-28 on S-protein RBD binding to heparin

RPI-27 and RPI-28 are sulfated heteropolysaccharides extracted from the brown seaweed, Saccharina japonica. The structure of these glycans are comprised of two varieties of polysaccharide frameworks: (1) a sulfated glucuronomannan and a glucuronomannan backbone consisting of 4-linked GlcA and 2-linked mannose (Man) repeats, along with a sulfated mannopyranose residue at the first C-6 position from the non-reducing end, (2) a glucuronan composed of GlcA units linked together in a 3-linked backbone. Several additional branched chains, including  $GlcA-(1\rightarrow 3)$ -Man- $(1\rightarrow 4)$ -GlcA.  $Man-(1\rightarrow 3)-GlcA-(1\rightarrow 4)-GlcA$ . Fuc- $(1\rightarrow 4)$ -GlcA, and Fuc- $(1\rightarrow 3)$ -Fuc. (Fig. 1) [34]. RPI-27 and RPI-28 share the same structure but have a different average molecular weight with 100 kDa and 12 kDa respectively.

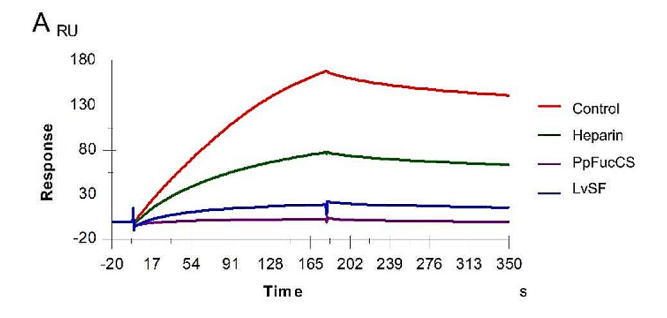
In this competition SPR analysis, RPI-27 and RPI-28 glycans (5 µg/mL) was premixed with 1 µM RBD of S-proteins (WT and XBB.1.5 individually). Solution competition results between these glycans and heparin are indicated in Fig. 7A, C. RPI-27 and RPI-28 exhibited high inhibition of WT RBD of S-protein binding to heparin, with 83.7% and

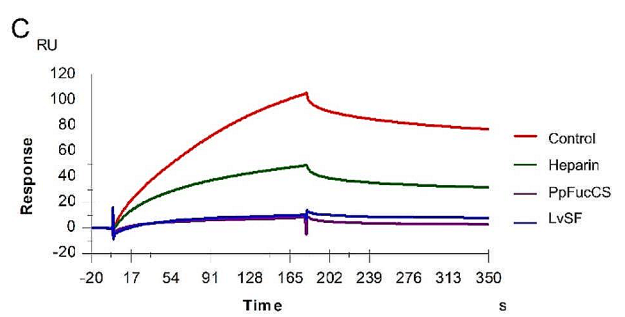


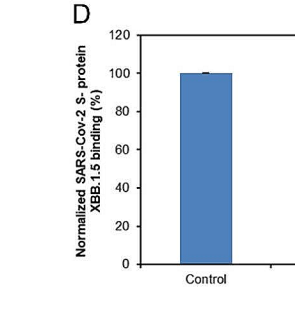
PoFucCS

PpFucCS

LvS







B 120

Normalized SARS-Cov-2 S- protein wild-type binding (%)

80

60

40

20

Control

Heparin

Heparin

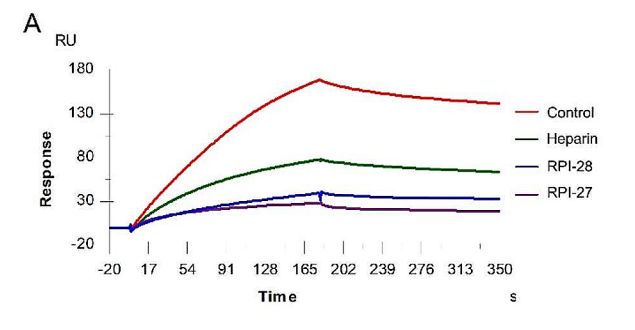
Fig. 6 Solution competition between heparin and PpFucCS and LvSF. (A) SPR sensorgrams of the WT SARS-CoV-2 S-protein RBD-heparin interaction competing with different PpFucCS and LvSF. The concentration of the WT SARS-CoV-2 S-protein RBD was 1  $\mu$ M mixed with 5  $\mu$ g/mL of different PpFucCS and LvSF glycans. (B) Bar graphs (based on triplicate experiments with standard deviation) of normalized WT SARS-CoV-2 S-protein RBD binding preference to surface heparin by competing with different PpFucCS and LvSF glycans. (C) SPR sensorgrams of the XBB.1.5 SARS-CoV-2 S-protein RBD-hepa-

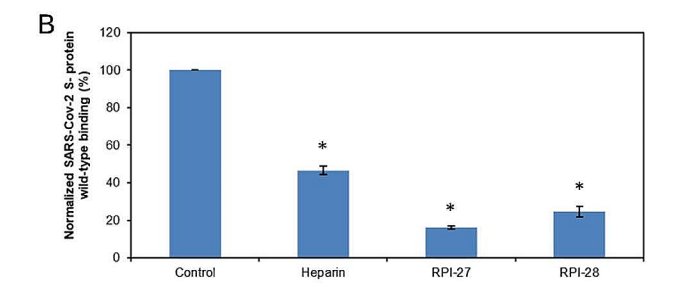
rin interaction competing with different PpFucCS and LvSF glycans. The concentration of the the XBB.1.5 SARS-CoV-2 S-protein RBD was 1  $\mu$ M mixed with 5  $\mu$ g/mL of different PpFucCS and LvSF glycans. **(D)** Bar graphs (based on triplicate experiments with standard deviations) of the normalized XBB.1.5 SARS-CoV-2 S-protein RBD binding preference to surface heparin by competing with different PpFucCS and LvSF glycans. Statistical analysis was performed using an unpaired two-tailed t-test (\*:  $p \le 0.05$  compared with the control)

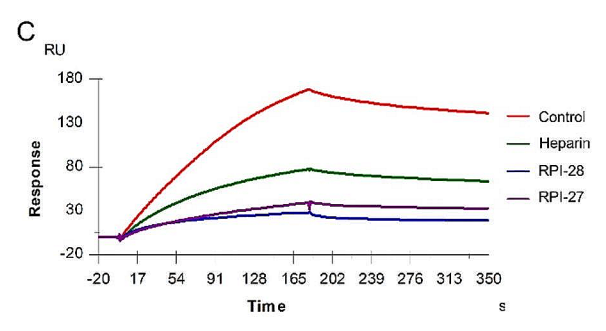
75.4%, respectively. Meanwhile, RPI-27 and RPI-28 also showed good inhibitions of XBB.1.5 RBD of S-protein binding to heparin, with 68.3% and 74.4%, respectively (Fig. 7B, D).

The inhibitory effects of all eight sulfated glycans derived from marine sources (IbSF, IbFucCS, HfSF, HfFucCS, PpFucCS, LvSF, RPI-27, PRI-28) were observed in their ability to inhibit the interactions between SARS-CoV-2 RBD of S-proteins (both WT and XBB.1.5) and heparin. Nonetheless, the binding activity of both RBD of S-proteins to surface-immobilized heparin was noticeably diminished in the chemically desulfated glycans (desIbSF and desIb-FucCS). Our study shows that sulfo group plays critical roles in the inhibitory activity of sulfated glycans derived from marine. The inhibition activity of all eight sulfated glycans sourced from the marine was remarkably effective in inhibiting the binding of surface-immobilized heparin with both wild-type and XBB.1.5 RBD of S-proteins. IbFucCS, out of the three distinct fucosylated chondroitin sulfates derived from marine sources, displayed the highest sulfation level (96% branching disulfated fucoses) and demonstrated best inhibitory activity against WT S-protein. HfFucCS (80% branching disulfated fucoses) shows slightly better inhibitory activity than PpFucCS (70% branching disulfated fucoses) against both WT and XBB.1.5. Clearly, sulfation levels/patterns are an important factor for the inhibitory activities of marine-sourced FucCS glycans. Despite sharing the same fucan tetrasaccharide repeating unit, IbSF, LvSF and HfSF differ in their sulfation patterns and are less sulfated than heparin. The higher sulfated LvSF has pentasulfated tetrasaccharide building blocks, while the building blocks of IbSF and HfSF consist of tetrasulfated tetrasaccharides. Among them, IbSF showed the highest inhibitory activity, while LvSF and HfSF exhibited comparable inhibitory activities. This suggests that sulfation pattern has a more pronounced effect on the interactions with S-proteins of SARS-Cov-2 than the degree of sulfation. Although HfSF and LvSF are not statistically different, but slightly weaker than IbSF, these marine sulfated glycans show statistically different (stronger) inhibitions as compared to heparin. RPI-27 and RPI-28 showed similar inhibitory activity, indicating that no obvious correlations between this seaweed-derived fucoidan molecular weight and binding properties. Despite the strong inhibitory activity of the binding properties of all the sulfated glycans evaluated against viral proteins in the SPR-based assay on surface-immobilized heparin do









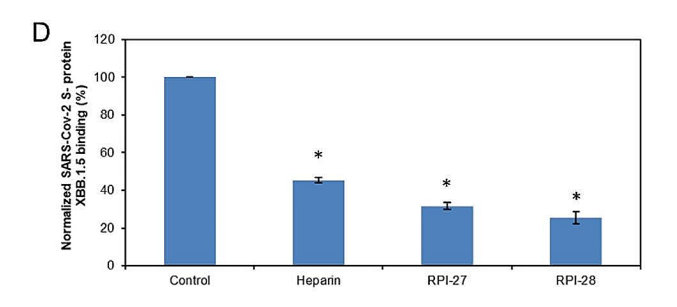


**Fig. 7** Solution competition between heparin and RPI-27/ RPI-28. **(A)** SPR sensorgrams of the WT SARS-CoV-2 S-protein RBD-heparin interaction competing with RPI-27/ RPI-28. The concentration of the WT SARS-CoV-2 S-protein RBD was 1μM mixed with 5 μg/mL of different RPI-27/ RPI-28 glycans. **(B)** Bar graphs (based on triplicate experiments with standard deviation) of normalized WT SARS-CoV-2 S-protein binding preference to surface heparin by competing with different RPI-27/ RPI-28 glycans. **(C)** SPR sensorgrams of the XBB.1.5 SARS-CoV-2 S-protein-heparin interaction competing

with different RPI-27/ RPI-28 glycans. The concentration of the the XBB.1.5 SARS-CoV-2 S-protein RBD was  $1\mu M$  mixed with 5  $\mu g/mL$  of different RPI-27/ RPI-28 glycans. (D) Bar graphs (based on triplicate experiments with standard deviations) of the normalized XBB.1.5 SARS-CoV-2 S-protein RBD binding preference to surface heparin by competing with different RPI-27/ RPI-28 glycans. Statistical analysis was performed using an unpaired two-tailed t-test (\*:  $p \le 0.05$  compared with the control)

not show any distinct correlations with their structural features. Our previous study revealed similar outcomes regarding the inhibitory effects of these sulfated glycans against other emerging SARS-CoV-2 variants and the Monkeypox virus [16]. It is known that sulfation levels (electronegativity density) are not the only factor for enhancing affinity for protein interactions. The overall structure found in the binding unit of the sulfated polysaccharide is the key factor regulating the binding quality. In fact, the addition of sulfate group(s) at certain sites of the composing monosaccharides of the binding units can lead to a deleterious outcome as shown before for the marine sulfated glycans in interactions with blood (co)-factors [35] and heparin hexasaccharides in interactions with fibroblast growth factor-1 [36].

It is well known that heparin binding proteins (HBP) require minimum chain size of heparin oligosaccharide and most of the interactions are chain size dependent. In our previous competition SPR studies using heparin oligosaccharides, indicated that high affinity binding of SARS-Cov-2 S-protein RBDs to heparin requires chain length greater than 18 [37]. The MWs of the marine sulfated glycans are the following: IbSF (≥100 kDa), IbFucCS (~75 kDa), HfSF (≥100 kDa), HfFucCS (~50 kDa), LvSF

(≥ 100 kDa), PpFucCS (~50 kDa) [15, 33, 38–39]. Generally speaking, the SF molecules have high MWs above hundred(s) of kDa while the FucCS molecules show MWs around 50–70 kDa. Since the MWs of all FucCS and SF molecules are commonly high, it is not believed that their MWs are dictating the distinct interactions with the omicron RBDs as seen in this work. Two fucoidans with different MWs: RPI-27 (MW~100 kDa) and RPI-28 (MW~12 kDa), but showed comparable inhibitory activity. In order to obtain a whole picture on the structure-activity relationship, more studies are needed to test the inhibitory activities using different sizes of oligosaccharides sulfated marine glycans in our future work.

IC<sub>50</sub> values for heparin, IbSF, IbFucCS and PpFucCS for inhibition of WT/XXB.1.5 S-protein-heparin were measured (Table 2 and supplemental Figure S1 and S2). The IC<sub>50</sub> values agree with the inhibition activities from the single concentration measurements.



Table 2 IC<sub>50</sub> values (ng/mL) of heparin, IbSF, IbFucCS and PpFucCS for inhibition on WT/XXB.1.5 S-protein RBD-heparin interaction

	Heparin	IbSF	IbFucCS	PpFucCS	HfSF	HfFucCS	LvSF	RPI27	RPI28
WT	31	17.4	6.7	6.1	23.6	20.5	22.3	25.6	28.1
	$(\pm 4.1)*$	$(\pm 2.2)*$	$(\pm 0.5)*$	$(\pm 0.4)*$	$(\pm 1.4)*$	$(\pm 2.1)*$	$(\pm 1.8)*$	$(\pm 2.3)*$	$(\pm 3.1)*$
XBB.1.5	27.6	16.9	10.5	9.7	20.6	21.8	19.0	25.1	23.2
	$(\pm 1.7)*$	$(\pm 1.2)*$	$(\pm 0.9)*$	$(\pm 0.7)*$	$(\pm 1.9)*$	$(\pm 1.6)*$	$(\pm 1.1)*$	$(\pm 2.6)*$	$(\pm 2.0)*$

<sup>\*</sup>Values were obtained through SPR measurements by analyzing the binding of S-protein RBD (WT or XBB.1.5) to surface heparin in competition with corresponding sulfated glycans. Standard deviations (±SD) were calculated based on triplicate SPR measurements

### **Conclusion**

SARS-CoV-2 RBD of S-proteins (WT and XBB.1.5) strongly bound to surface immobilized heparin. SPR competition assays were conducted to analyze the solution competition between heparin immobilized on the surface and ten sulfated glycans from marine sources (IbSF, desIbSF, IbFucCS, desIbFucCS, PpFucCS, LvSF, HfSF, HfFucCS, RPI-27 and RPI-28). Our finding demonstrated that all the eight naturally occurring marine-sourced sulfated glycans (IbSF, IbFucCS, PpFucCS, LvSF, HfSF, HfFucCS, RPI-27 and RPI-28) provided striking inhibitory activity of chipsurface heparin binding to the WT and XBB.1.5 RBD of S-proteins, whereas the inhibitory activity of chemically desulfated IbSF IbFucCS (desIbSF and desIbFucCS) were found to be very low. This data reveals that the sulfated glycans derived from sea cucumbers and seaweed exhibit great potential as natural inhibitors of evolving variants of SARS-CoV-2 by efficiently attaching to viral S-proteins. The study of molecular interactions, particularly the degree of sulfation, will pave the way for developing novel therapeutic approaches to prevent and treat the rapidly evolving SARS-CoV-2 disease. To further approve the antiviral therapeutic potential of these sulfated marine glycans, detailed structure-activity relationship, cell-based assay (in vitro) and animal-based (in vivo) evaluation are proposed in our future study.

**Supplementary Information** The online version contains supplementary material available at https://doi.org/10.1007/s10719-024-10150-1.

**Author contributions** Conceptualization, F.Z. and R.J.L.; methodology, P.H, D.S.; analysis, P.H, Y.L.; resource, S.K., R.D., V.H.P., M.F.; W.J.; J.B; preparation of original draft, P.H, Y.L., F.Z; draft review and draft editing, K.X., V.H.P., J.B.; J.S.D. and R.J.L.; draft revision, P.H., V.H.P., F.Z. and R.J.L., acquisition of funding, J.S.D., V.H.P., C.W., F.Z. and R.J.L.

Funding This work was supported by NIH (S10OD028523 and R21AI156573 (R.J.L, F.Z.), 1P20GM130460-01A1-7936 and 1R03NS110996-01A1 (V.H.P.), R01 AG069039-01 (C.W.)); National Science Foundation GlycoMIP, DMR-1933525 (R.J.L., J.S.D., F.Z.), and New York State Biodefense Commercialization Fund (J.S.D., F.Z).

Data availability No datasets were generated or analysed during the current study.

### **Declarations**

Conflict of interest The authors state that they have no conflicts of interest.

### References

- Bakhshandeh, B., Jahanafrooz, Z., Abbasi, A., Goli, M.B., Sadeghi, M., Mottaqi, M.S., Zamani, M.: Mutations in SARS-CoV-2; consequences in structure, function, and pathogenicity of the virus. Microb. Pathog. 154, 104831 (2021). https://doi. org/10.1016/j.micpath.2021.104831
- Zhou, Y., Zhi, H., Teng, Y.: The outbreak of SARS-CoV-2 omicron lineages, immune escape, and vaccine effectivity. J. Med. Virol. 95 (2023). https://doi.org/10.1002/jmv.28138 e28138
- Qu, P., Faraone, J.N., Evans, J.P., Zheng, Y.-M., Carlin, C., Anghelina, M., Stevens, P., Fernandez, S., Jones, D., Panchal, A.R., Saif, L.J., Oltz, E.M., Zhang, B., Zhou, T., Xu, K., Gumina, R.J., Liu, S.-L.: Enhanced evasion of neutralizing antibody response by Omicron XBB.1.5, CH.1.1, and CA.3.1 variants. Cell. Rep. 42, 112443 (2023). https://doi.org/10.1016/j.celrep.2023.112443
- Uriu, K., Ito, J., Zahradnik, J., Fujita, S., Kosugi, Y., Schreiber, G., Sato, K.: Enhanced transmissibility, infectivity, and immune resistance of the SARS-CoV-2 omicron XBB.1.5 variant. Lancet Infect. Dis. 23, 280–281 (2023). https://doi.org/10.1016/ S1473-3099(23)00051-8
- Gandhi, N.S., Mancera, R.L.: The structure of glycosaminoglycans and their interactions with proteins. Chem. Biol. Drug Des. 72, 455– 482 (2008). https://doi.org/10.1111/j.1747-0285.2008.00741.x
- Kamhi, E., Joo, E.J., Dordick, J.S., Linhardt, R.J.: Glycosaminoglycans in infectious disease. Biol. Rev. 88, 928–943 (2013). https://doi.org/10.1111/brv.12034
- Aquino, R.S., Park, P.W.: Glycosaminoglycans and infection. Front. Biosci. 21, 1260–1277 (2016). https://doi.org/10.2741/4455
- Chittum, J.E., Sankaranarayanan, N.V., O'hara, C.P., Desai, U.R.:
  On the selectivity of Heparan Sulfate Recognition by SARS-CoV-2 Spike Glycoprotein. ACS Med. Chem. Lett. 12, 1710–1717 (2021). https://doi.org/10.1021/acsmedchemlett.1c00343
- Yan, L., Song, Y., Xia, K., He, P., Zhang, F., Chen, S., Pouliot, R., Weiss, D.J., Tandon, R., Bates, J.T., Ederer, D.R., Mitra, D., Sharma, P., Davis, A., Linhardt, R.J.: Heparan sulfates from bat and human lung and their binding to the spike protein of SARS-CoV-2 virus. Carbohydr. Polym. 260, 117797 (2021). https://doi. org/10.1016/j.carbpol.2021.117797
- Kearns, F.L., Sandoval, D.R., Casalino, L., Clausen, T.M., Rosenfeld, M.A., Spliid, C.B., Amaro, R.E., Esko, J.D.: Spike-heparan sulfate interactions in SARS-CoV-2 infection. Curr. Opin. Struct. Biol. 76, 102439 (2022). https://doi.org/10.1016/j.sbi.2022.102439
- Kang, H.-K., Seo, C.H., Park, Y.: The effects of Marine Carbohydrates and Glycosylated compounds on Human Health. Int. J. Mol. Sci. 16, 6018–6056 (2015)



- Arokiarajan, M.S., Thirunavukkarasu, R., Joseph, J., Ekaterina, O., Aruni, W.: Advance research in biomedical applications on marine sulfated polysaccharide. Int. J. Biol. Macromol. 194, 870– 881 (2022). https://doi.org/10.1016/j.ijbiomac.2021.11.142
- Kwon, P.S., Oh, H., Kwon, S.-J., Jin, W., Zhang, F., Fraser, K., Hong, J.J., Linhardt, R.J., Dordick, J.S.: Sulfated polysaccharides effectively inhibit SARS-CoV-2 in vitro. Cell. Disc. 6, 50 (2020). https://doi.org/10.1038/s41421-020-00192-8
- Song, Y., He, P., Rodrigues, A.L., Datta, P., Tandon, R., Bates, J.T., Bierdeman, M.A., Chen, C., Dordick, J., Zhang, F., Linhardt, R.J.: Anti-SARS-CoV-2 activity of Rhamnan Sulfate from Monostroma Nitidum. Mar. Drugs. 19, 685 (2021)
- Dwivedi, R., Sharma, P., Farrag, M., Kim, S.B., Fassero, L.A., Tandon, R., Pomin, V.H.: Inhibition of SARS-CoV-2 wild-type (Wuhan-Hu-1) and Delta (B.1.617.2) strains by marine sulfated glycans. Glycobiology. 32, 849–854 (2022). https://doi.org/10.1093/glycob/cwac042
- He, P., Shi, D., Li, Y., Xia, K., Kim, S.B., Dwivedi, R., Farrag, M., Pomin, V.H., Linhardt, R.J., Dordick, J.S., Zhang, F.: SPR Sensor-Based Analysis of the Inhibition of Marine Sulfated Glycans on Interactions between Monkeypox Virus Proteins and Glycosaminoglycans. Mar. Drugs 21, 264 (2023) (2023)
- Guo, D., Duan, H., Cheng, Y., Wang, Y., Hu, J., Shi, H.: Omicron-included mutation-induced changes in epitopes of SARS-CoV-2 spike protein and effectiveness assessments of current antibodies. Mol. Biomed. 3, 12 (2022). https://doi.org/10.1186/s43556-022-00074-3
- Wang, Q., Iketani, S., Li, Z., Liu, L., Guo, Y., Huang, Y., Bowen, A.D., Liu, M., Wang, M., Yu, J., Valdez, R., Lauring, A.S., Sheng, Z., Wang, H.H., Gordon, A., Liu, L., Ho, D.D.: Alarming antibody evasion properties of rising SARS-CoV-2 BQ and XBB subvariants. Cell. 186, 279–286 (2023). https://doi.org/10.1016/j. cell.2022.12.018
- Yamasoba, D., Uriu, K., Plianchaisuk, A., Kosugi, Y., Pan, L., Zahradnik, J., Ito, J., Sato, K.: Virological characteristics of the SARS-CoV-2 omicron XBB.1.16 variant. Lancet Infect. Dis. 23, 655–656 (2023) (2023). https://doi.org/10.1016/ S1473-3099(23)00278-5
- Muñoz, E.M., Linhardt, R.J.: Heparin-binding domains in Vascular Biology. Arterioscler. Thromb. Vasc Biol. 24, 1549–1557 (2004). https://doi.org/10.1161/01.ATV.0000137189.22999.3f
- Weiss, R.J., Esko, J.D., Tor, Y.: Targeting heparin and heparan sulfate protein interactions. Org. Biomol. Chem. 15, 5656–5668 (2017). https://doi.org/10.1039/C7OB01058C
- Kim, S.Y., Jin, W., Sood, A., Montgomery, D.W., Grant, O.C., Fuster, M.M., Fu, L., Dordick, J.S., Woods, R.J., Zhang, F., Linhardt, R.J.: Characterization of heparin and severe acute respiratory syndrome-related coronavirus 2 (SARS-CoV-2) spike glycoprotein binding interactions. Antiviral Res. 181, 104873 (2020). https://doi.org/10.1016/j.antiviral.2020.104873
- Clausen, T.M., Sandoval, D.R., Spliid, C.B., Pihl, J., Perrett, H.R., Painter, C.D., et al.: SARS-CoV-2 infection depends on cellular heparan sulfate and ACE2. Cell. 183, 1043–1057 (2020). https://doi.org/10.1016/j.cell.2020.09.033 e15
- Shafti-Keramat, S., Handisurya, A., Kriehuber, E., Meneguzzi, G., Slupetzky, K., Kirnbauer, R.: Different Heparan Sulfate proteoglycans serve asCellular receptors for HumanPapillomaviruses. J. Virol. 77, 13125–13135 (2003). https://doi.org/10.1128/jvi.77.24.13125-13135.2003
- De Pasquale, V., Quiccione, M.S., Tafuri, S., Avallone, L., Pavone, L.M.: Heparan Sulfate proteoglycans in viral infection and treatment: A special focus on SARS-CoV-2. Int. J. Mol. Sci. 22, 6574 (2021)
- Shi, D., Bu, C., He, P., Song, Y., Dordick, J.S., Linhardt, R.J., Chi, L., Zhang, F.: Structural Characteristics of Heparin Binding

- to SARS-CoV-2 spike protein RBD of Omicron sub-lineages BA.2.12.1, BA.4 and BA.5. Viruses. 14, 2696 (2022)
- Shi, D., He, P., Song, Y., Linhardt, R.J., Dordick, J.S., Chi, L., Zhang, F.: Interactions of heparin with key glycoproteins of human respiratory syncytial virus. Front. Mol. Biosci. 10 (2023). https://doi.org/10.3389/fmolb.2023.1151174
- Chen, S., Hu, Y., Ye, X., Li, G., Yu, G., Xue, C., Chai, W.: Sequence determination and anticoagulant and antithrombotic activities of a novel sulfated fucan isolated from the sea cucumber Isostichopus badionotus. Biochim. Biophys. Acta (BBA) Gen. Subj. 1820, 989–1000 (2012). https://doi.org/10.1016/j.bbagen.2012.03.002
- Chen, S., Xue, C., Yin, L.A., Tang, Q., Yu, G., Chai, W.: Comparison of structures and anticoagulant activities of fucosylated chondroitin sulfates from different sea cucumbers. Carbohydr. Polym. 83, 688–696 (2011). https://doi.org/10.1016/j.carbpol.2010.08.040
- Castro, M.O., Pomin, V.H., Santos, L.L., Vilela-Silva, A.-C.E.S., Hirohashi, N., Pol-Fachin, L., Verli, H., Mourão, P.S.: A unique 2-Sulfated β-Galactan from the Egg Jelly of the Sea Urchin Glyptocidaris Crenularis. J. Biol. Chem. 284, 18790–18800 (2009). https://doi.org/10.1074/jbc.M109.005702
- Shi, D., Qi, J., Zhang, H., Yang, H., Yang, Y., Zhao, X.: Comparison of hydrothermal depolymerization and oligosaccharide profile of fucoidan and fucosylated chondroitin sulfate from Holothuria floridana. Int. J. Biol. Macromol. 132, 738–747 (2019). https://doi.org/10.1016/j.ijbiomac.2019.03.127
- 32. Mulloy, B., Ribeiro, A.C., Alves, A.P., Vieira, R.P., Mourão, P.A.: Sulfated fucans from echinoderms have a regular tetrasaccharide repeating unit defined by specific patterns of sulfation at the 0–2 and 0–4 positions. J. Biol. Chem. **269**, 22113–22123 (1994). https://doi.org/10.1016/S0021-9258(17)31763-5
- Dwivedi, R., Samanta, P., Sharma, P., Zhang, F., Mishra, S.K., Kucheryavy, P., Kim, S.B., Aderibigbe, A.O., Linhardt, R.J., Tandon, R., Doerksen, R.J., Pomin, V.H.: Structural and kinetic analyses of holothurian sulfated glycans suggest potential treatment for SARS-CoV-2 infection. J. Biol. Chem. 297 (2021). https://doi.org/10.1016/j.jbc.2021.101207
- Jin, W., Wang, J., Ren, S., Song, N., Zhang, Q.: Structural analysis of a Heteropolysaccharide from Saccharina Japonica by Electrospray Mass Spectrometry in Tandem with Collision-Induced Dissociation Tandem Mass Spectrometry (ESI-CID-MS/MS). Mar. Drugs. 10, 2138–2152 (2012)
- Pomin, V.H.: Anticoagulant motifs of marine sulfated glycans. Glycoconj. J. 31, 341–344 (2014). https://doi.org/10.1007/s10719-014-9530-1
- Muñoz-García, J.C., García-Jiménez, M.J., Carrero, P., Canales, A., Jiménez-Barbero, J., Martín-Lomas, M., Imberty, A., de Paz, J.L., Angulo, J., Lortat-Jacob, H., Nieto, P.M.: Importance of the polarity of the glycosaminoglycan chain on the interaction with FGF-1. Glycobiology. 24, 1004–1009 (2014). https://doi. org/10.1093/glycob/cwu071
- Gelbach, A.L., Zhang, F., Kwon, S.J., Bates, J.T., Farmer, A.P., Dordick, J.S., Wang, C., Linhardt, R.J.: Interactions between heparin and SARS-CoV-2 spike glycoprotein RBD from omicron and other variants. Front. Mol. Biosci. 9, 912887 (2022). https:// doi.org/10.3389/fmolb.2022.912887
- Zoepfl, M., Dwivedi, R., Kim, S.B., McVoy, M.A., Pomin, V.H.: Antiviral activity of marine sulfated glycans against pathogenic human coronaviruses. Sci. Rep. 13, 4804 (2023). https://doi. org/10.1038/s41598-023-31722-5
- Farrag, M., Dwivedi, R., Sharma, P., Kumar, D., Tandon, R., Pomin, V.H.: Structural requirements of Holothuria floridana fucosylated chondroitin sulfate oligosaccharides in anti-SARS-CoV-2 and anticoagulant activities. PLoS One. 18, e0285539 (2023). https://doi.org/10.1371/journal.pone.0285539



**Publisher's Note** Springer Nature remains neutral with regard to jurisdictional claims in published maps and institutional affiliations.

Springer Nature or its licensor (e.g. a society or other partner) holds exclusive rights to this article under a publishing agreement with the author(s) or other rightsholder(s); author self-archiving of the accepted manuscript version of this article is solely governed by the terms of such publishing agreement and applicable law.

